FR8100449

1980 Annual conference condensed matter division of the
European physical society.
Anvers, Belgique, April 9 - 11, 1980.

CEA - CONF 5460

HIGH ENERGY ELECTRON MULTIBEAM DIFFRACTION AND IMAGING

Alain Bourret
Centre d'Etudes Nucléaires de Grenoble
Département de Recherche Fondamentale
Section de Physique du Solide
85 X 38041 GRENOBLE Cédex (France)

INTRODUCTION

Different particles have been used to explore the atomic or electronic structure of materials the principle among which are X rays, neutrons, electrons. Although electron diffraction was discovered 50 years ago nearly simultaneously with X rays, electron diffraction was not so widely used as X ray diffraction for structural studies. Apart from the important developpement by Vainshtein [1] for structure determination the contribution of electron diffraction was by no means small. This was due to a number of disadvantages which were difficult to ovecome in the past : the interaction between electrons and matter is very strong thus all the simple approximations employed for X rays fail and an electron diffraction pattern cannot be interpreted directly. As a consequence the "transparency" of matter to electrons is very limited and only very thin specimens can be explored (~ 100 to 1000 Å). In this geometrical form it is difficult to obtain sufficiently uniform sample (thickness and orientation) to produce valid results. Furthermore some materials are radiation sensitive and rapidly destroyed under the electron beam.

In the last decade however a remarkable development of electron diffraction and imaging methods has occurred. Complicated structures were directly solved on images at a 2-3 Å level [2] since the early work on oxides structure done by Cowley and Iijima [3]. Important experimental progress was also made in the investigation of the "optical" potential seen by electrons extending the interest from crystallography to solid state physics. In addition the recent development of modern electron microscopes (scanning

or transmission electron microscope) offers the enormous advantage of obtaining structural information localized at a level never previously attainable : microdiffraction pattern from region of 10 Å are now possible and structural defects are explored at an atomic level. Owing to the instrumental versatility diffraction and images can also be complemented in a way which minimizes the electron dose and ovecomes partially the radiation problem for sensitive material [6]. This recent development has been mainly favored by the emergence of good theories of dynamical scattering and the ease of obtaining computed solutions. As a consequence it appears that strong dynamical scattering of electrons is not at all an inconvenient but can be an advantage to explore in more detail atomic or electronic structures.

Many recent reviews of dynamical electron scattering and its application have recently appeared. Two of them give an overall survey of the subject : "Electron diffraction 1927-1977" from papers given at the International Conference on Electron Diffraction in 1977 [4] and the Nobel Symposium on Direct imaging of Atomic in Crystals and Molecules [5]. The present contribution will be limited to high energy electrons (> 50 keV) as low energy electron diffraction (LEED) needs a specific approach and offers at present no possibility of combining diffraction and images.

The different theories of dynamical scattering of electrons will firstly be reviewed with special reference to their basis and the validity of the different approximations. Then after a short description of the different experimental set ups, structural analysis and the investigation of the "optical" potential by means of high energy electrons will be surveyed.

THEORY OF DYNAMICAL SCATTERING OF ELECTRONS

Although the basis of dynamical scattering theory was already in place two decades ago this domain is still active in many respects : in particular the definition of the potential seen by high energy electrons and the search for adequate approximations to obtain either an invertible form or an analytical solution. The basis of the different formulations which are presented, must first be clarified.

The basis of dyanmical scattering

The propagation of high energy electrons is generally described by the Schrödinger equation :

$$\left[\nabla^2 + 4\pi^2 k^2 - \frac{2mV(\underset{\sim}{r})}{\hbar^2}\right] \psi(\underset{\sim}{r}) = 0 \qquad (1)$$

where k is the wave vector. The solution of (1) with the appropriate boundary conditions would describe the complete scattering of electrons. In fact (1) is a considerable restriction of the general problem : it describes only one particle propagating in a potential $V(\underset{\sim}{r})$ having no internal degrees of freedom. Therefore inelastic scattering of the electron beam by matter is entirely neglected. Although dynamical inelastic scattering can be deduced from a time dependent Schrödinger equation as in the form proposed by Yoshioka [7] very little work has been done in this direction [8]. However (1) can describe adequately the elastic scattering if and only if :

i) The potential $V(\underset{\sim}{r})$ is complex to allow for the absorption of elastically electrons by inelastic processes. This phenomenologic treatment has been justified on the basis of more elaborate theories by Yoshioka [7] and others [9] : $V^{opt}(\underset{\sim}{r}) = V(\underset{\sim}{r}) + iV'(\underset{\sim}{r})$. This potential has been called the "optical" potential by analogy with the use of a complex dielectric constant in optics or X ray diffraction. Various attempts have been made to understand the physical meaning of the real and the imaginary part of this potential, and to make good estimates of them. In principle the <u>real part</u> $V(\underset{\sim}{r})$ would represent the Coulomb interaction and the exchange however the exchange term is negligible for high energy electron [10], and the crystal is essentially coulombic and so the electrons see the total crystal potential including solid state bonding effects, exchange and correlation effects between electrons in the crystal structure. Therefore the Born atomic structure factor often use in the description of the real part is only a first approximation, and more accurate results must also include bonding effects. The <u>imaginary part</u> $V'(\underset{\sim}{r})$ is characterized in a crystal by its Fourier coefficients V'_o and V'_g corresponding to the g^{th} diffraction vector. The central part V'_o describes the background absorption with a mean free path Λ^o: the complex dielectric constant gives a good estimate of this term, and V'_o represents mainly collective excitations such as plasmons [11]. On the other hand the anomalous part V'_g arises mainly from thermal diffuse scattering by phonons as shown by Hall and Hirsch [12]. Generally the orders of magnitude are such that $V'(\underset{\sim}{r}) \sim 0.1\ V(r)$.

ii) Thermal atomic vibrations, already included in the imaginary part, affect also the real part. An average potential $< V(\underset{\sim}{r}) >$ is usually introduced by convolution with the probability density function for thermal vibrations. In a crystal the Fourier coefficients V_g are then affected by the usual Debye Waller factor. Exact dynamical calculations of vibrating crystals do not as yet exist, although it is possible to computer simulate it on the multislice method (see below).

iii) Relativistic effects are included as the rest mass energy of electrons (511 keV) is comparable to the kinetic energy.

Thus relativistic expressions for m and $\underset{\sim}{k}$ have to be used.

One further simplification is usually made with high energy electrons : the forward scattering approximation. As the electron wavelenght is much smaller than interatomic distances the scattering is strongly favored in the forward direction. Then if z is along the electron beam direction substituting :

$$\psi(\underset{\sim}{r}) = \exp(2\pi i k z)\ \tau(\underset{\sim}{r},z)$$

and neglecting second derivatives in z of τ, (1) becomes :

$$4\pi i k \frac{\partial \tau}{\partial z} = [-\nabla_r^2 + \frac{2mV(\underset{\sim}{r},z)}{\hbar^2}]\tau(\underset{\sim}{r},z) \qquad (2)$$

which will serve as the starting equations for dynamical scattering. Two major approaches have been developped for solving (2) in a periodic or, even non periodic potential : the Bloch wave method, and the coupled plane wave theories based on Darwin's treatment [13].

The Bloch wave method

Generalyzing the first treatment of dynamical electron diffraction by Bethe [14] in a crystal, a solution of (2) is expressed as a sum of N two dimensionnal Bloch waves each Bloch wave being described by a sum of plane waves :

$$\psi_j(\underset{\sim}{r}) = \sum_g C_g^{(j)} e^{2\pi i\, \underset{\sim}{k}^{(j)} \cdot \underset{\sim}{r}} e^{2\pi i \underset{\sim}{g}\cdot\underset{\sim}{r}} \qquad (3)$$

Since the Bloch waves all have the same energy (k^2), and the same transverse component to match the boundary condition at the entrance surface only the z component of $\underset{\sim}{k}^{(j)}$ differ from one Bloch wave to the other. The termination of the $\underset{\sim}{k}^{(j)}$ vectors will describe the dispersion surface with a number of branches equal to the total number of Bloch wave considered (see fig. 1). Let :

$$\gamma_j = k_z^{(j)} - k_z \qquad (4)$$

then from (2) amplitude and wave vector of the Bloch waves are given by solving the equation :

$$\sum_{g'} \{(\gamma_j + S_g)\ \delta_{gg'} + \frac{m}{h^2 k} V_{g-g'}\}\ C_g^{(j)} = 0 \qquad (5)$$

where S_g is the distance in the z direction from the Ewald sphere

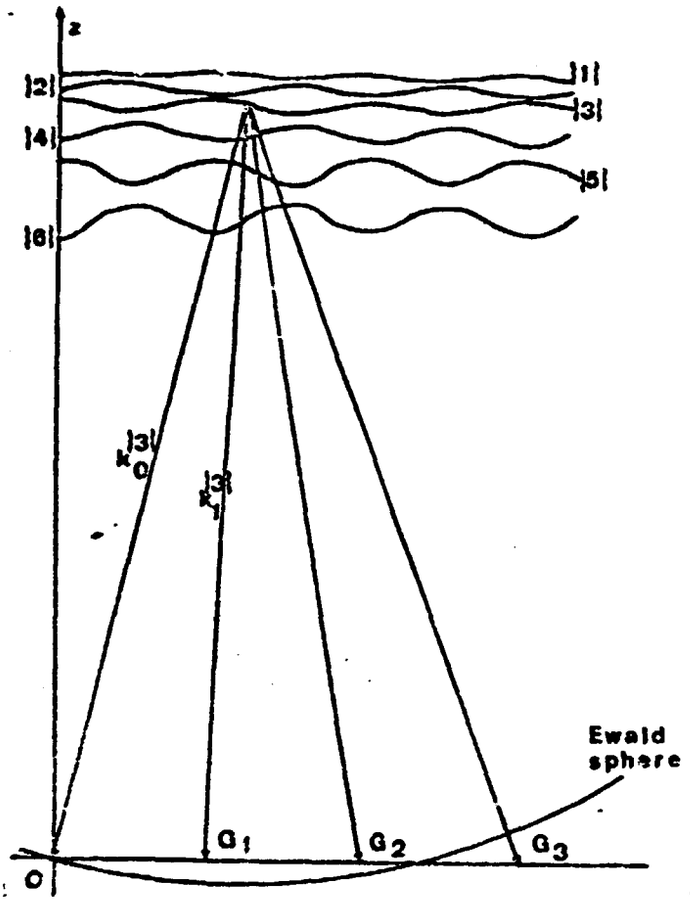

Fig. 1 - Dispersion surface giving the loci of the wave vector propagating in a crystal. This surface has been limited to six branches.

to the reciprocal lattice point g. The multibeam equations (5) are of standard eigenvalue form and for solving (5) it is necessary to diagonalize one particular matrix M. The general solution of (2) is then given by a linear combination of Bloch waves whose excitations are calculated by expressing the boundary conditions. The resulting wave at the exit face is then given by :

$$\psi_T = \sum_g \sum_{j=1}^{N} C_o^{(j)} C_g^{(j)} \exp 2\pi i \gamma^{(j)} t \exp 2\pi i \underset{\sim}{g}.\underset{\sim}{r} \qquad (6)$$

The diagonalization of the matrix involved in (5) can give an analytical solution for only a few beams in general 3 unless particular symmetry conditions would allow appropriate reduction of M.

The effect of the imaginary part of the potential is often calculated by a perturbation method as $V'(\underset{\sim}{r})$ is always smaller than $V(\underset{\sim}{r})$. It introduces a complex eigen value $\gamma^{(j)}$ the imaginary part of which corresponds to an attenuation different for each Bloch wave : this is known as the anomalous absorption effect and is identical to the Borrmann effect for X rays, in particular attenuation is more pronounced for symmetric Bloch waves.

For computation the number of beams must be limited to the lowest compatible with experimental accuracy. As the method is self consistent whatever the beam number, the square modulus of the total wave is constant when absorption is neglected. A practical means to determine the appropriate number of beams to use is to increase the number of beams until a stationary value of eigen values is reached.

Generally speaking this number increases with the voltage and depends strongly on the specimen orientation (via the S_g parameters in (5)). A relatively small number (3 to 20) is necessary when the Ewald sphere is close to one row of the reciprocal space, but many more beams are necessary (50-1000) when the Ewald sphere is close to a dense plane of the reciprocal space i.e. when the beam is aligned along a low index row of the crystal. This would give particularly lengthy calculation unless fast computer is used. An example of such calculation in fig. 2 gives the phase and amplitude of the central beam and of one diffracted beam at the exit face of a germanium slice as a function of its thickness.

The coupled plane wave theories (Darwin type)

Following the Darwin method [13] it is useful to write the electron wave in the material as a sum of coupled plane wave the amplitudes of which vary with position, instead of a sum of independent Bloch waves. Thus as proposed by Howie and Whelan [17] the wave function inside a crystal is written :

$$\psi(\underset{\sim}{r},z) = \sum_g a_g(z) \exp 2\pi i \underset{\sim}{k}.\underset{\sim}{r} \exp 2\pi i \underset{\sim}{g}.\underset{\sim}{r} \qquad (7)$$

and from (2) the amplitudes must satisfy :

$$\frac{da_g}{dz} = -2\pi i S_g a_g - \frac{im}{\pi k \hbar^2} \sum_{g'} V_{g-g'} a_{g'} \qquad (8)$$

This coupled system of equations can be formally integrated [18] in the form :

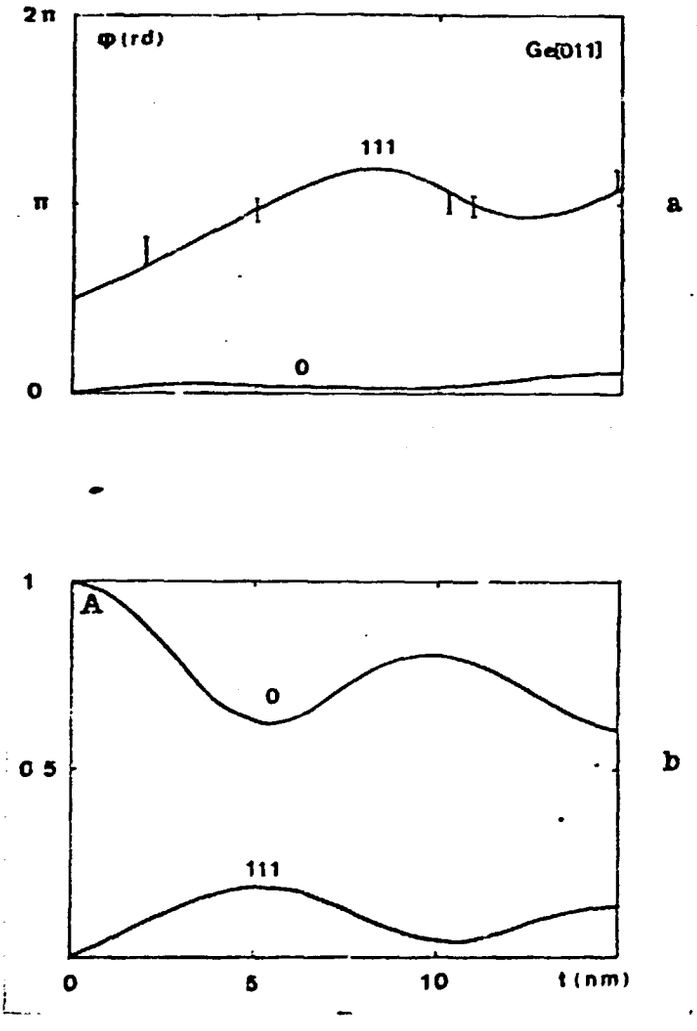

Fig. 2 - Calculated amplitudes and phases of 0 and 111 beams in germanium oriented along [011] axis. Experimental data for phases as measured from direct atomic high resolution images are compared to the calculated values. Dynamical calculation ; 156 beams by Bloch waves method including absorption.

$$a(z) = (\exp - i \frac{z}{2k} M)\, a(o) = S\, a(o) \qquad (9)$$

where a(z) is a column vector of the N amplitudes and S the scattering matrix. Exact calculation of S however is difficult and a

series expansion of (9) is of low convergence, therefore another form is generally prefered.

In the multislice formulation the description of propagation in the solid is made by dividing the solid into thin slices perpendicular to the electron beam and calculating the transmission of one slice. Successive application is performed the entrance conditions for the n + 1 slice being furnished by the exit wave function of the n slice.

It has been shown directly [15] from the Schrödinger equation (2) or from its integral form [16] that the effect of one slice is given in the limit of $\Delta z \to 0$, by :

$$\psi(\underset{\sim}{r},\Delta z) = P(\Delta z) * \{[\exp - \frac{i}{2\pi k}\frac{m}{\hbar^2}\bar{V}^{opt}(\underset{\sim}{r})\Delta z]\psi(\underset{\sim}{r},o)\} \qquad (10)$$

$m/2\pi kh^2$ is called the interaction constant σ, and is equal to $\pi/\lambda E$ where E is the electron energy, $P(\Delta z)$ is the Fresnel propagation function over Δz, and $*$ denotes the convolution product and $\bar{V}^{opt}(\underset{\sim}{r})$ the mean projected potential over Δz.

Successive applications of (10) will give a very good approximation of the dynamical scattering problem if the slice thickness is small enough. This thickness is usually taken as of the order of the lattice parameter along z unless the diffraction effect coming from upper layer Laue zone must be taken into account.

If applied to a periodic potential, (10) can be expressed as a finite sum of combinations of diffracted beams. The number of beams to be introduced in the theory is also determined empirically. The constancy of the square modulus $|\psi_r|^2$ when absorption is neglected is a criterium often used as this theory is not self consistent.

The convolution product is also for practical computation replaced by multiplication of the Fourier transforms : the Fast Fourier Transform algorithm has given a definite advantage to this method and problems including up to 10000 beams can be handle relatively easily.

Extension to non periodic potential

It is possible to extend the previous analysis to non periodic potentials. Most effort in the past was devoted to defects in periodic structures, so that the periodic character of the specimen is predominent. First order perturbation theory [19] on the Bloch wave approach has been proved to be relatively inadequate for high energy electrons and it is the coupled plane wave formulation which has been the most fruitful.

The theory developped by Howie and Whelan [17] is based on the column approximation i.e. that the amplitudes of the plane waves a_g are slowly varying with r. The result is very similar to (8) but using a "local" deviation parameter $S_g + \beta_g(r)$ instead of S_g where :

$$\beta_g(r) = \underset{\sim}{g} \cdot \frac{d\underset{\sim}{R}}{dz} \qquad (11)$$

with $\underset{\sim}{R}$ = local displacement of the lattice, and modified amplitudes $a'_g = a_g \exp 2\pi i \underset{\sim}{g}.\underset{\sim}{R}$.

This type of calculation has been widely used for calculating the contrast of linear or planar defects at low resolution and very limited number of beams [18]. A more refined treatment was made by Howie and Basinsky [20] without the column approximation and therefore is valid irrespective of the degree of distorsion of the crystal. However the coupled differential equations include second derivatives of wave function amplitude and they are cumbersome to integrate especially for high beam numbers [21].

More recently the development of high resolution has required a new approach based on the multislice theory. The propagation of the electron wave given by (10) is valid irrespective of the exact form of the potential $\bar{V}(r)$. Therefore in the non periodic case the convolution product can be performed by discrete sampling of V(r) which is equivalent to indroducing an artificially periodic crystal : this method is known as periodic continuation and has been successfully employed near point defects [22] or dislocations [23].

The different approximations to dynamical scattering

Although tne dynamical elastic scattering has been formerly solved by one of the equation sets (5), (8) or (10) and can effectively be calculated on modern computers, a constant effort has been applied to the search of adequate approximations which are in analytical form.

The simplest one, but of no real interest with electrons, is the kinematical approximation similar to the first Born approximation [24]. It states that the scattered waves are weak compared with the incident wave : it can be clearly interpreted as corresponding to a single scattering process. For an incident plane wave of amplitude unity the electron wave is then given simply by :

$$\psi(\underset{\sim}{r}) = 1 - i\frac{\pi}{\lambda E}\int_0^z V(\underset{\sim}{r},z')dz' = 1 - i\frac{\pi}{\lambda E}\bar{V}(\underset{\sim}{r})\,z \qquad (12)$$

and $\bar{V}(\underset{\sim}{r})$ is the mean projected potential at the point r. This ap-

proximation only holds for :

$$t < \frac{E\lambda}{\pi \bar{V}(\underset{\sim}{r})}$$

At high resolution (d $\sim$ 2 or 3 Å) where regions of high potential are explored this approximation is limited to specimen only a few atoms thick. In case of a large Z value, this approximation even fails for one atomic layer. Therefore although of great simplicity this weak phase object approximation is limited to very thin specimen of light atoms or to resolution larger than the mean projected distance between atoms. Higher electron energy would not improve very much the situation as λE tends to a limit hc/2 due to relativistic effects.

The second and more useful approximation is the phase object approximation. Since the wavelength of an electron is very small compared to the atomic distance and that the object potential vary only slowly over one wavelength the electron can be considered to follow the classical path i.e. a straight line through the object. Jap and Glaeser [25] have shown that unlike the first Born approximation, the phase object approximation takes multiple scattering processes into account but the scattered waves are supposed to propagate in the same direction parallel to the incident electron wave. The electron wave is given by :

$$\psi_T(\underset{\sim}{r}) = \exp[-\, i \frac{\pi}{\lambda E} \int_0^z V(\underset{\sim}{r},z')\, dz'] \qquad (13)$$

This equation follows directly from integration of (2) when ∇_r^2 is neglected. The condition for the validity of (13) can be written :

$$z << \frac{2d_{min}^2}{\lambda} \qquad (14)$$

where d_{min} is the minimum resolvable distance. (14) states that the path length between the straight line parallel to the incident beam and to the more inclined scattered beam is smaller than the electron wavelength. Thickness as deduced from (14) is typically of the order of 50 Å and therefore can be useful in case of high resolution studies where specimen thickness is anyway limited to avoid chromatic aberration.

A higher order phase object approximation in an invertible form has been recently proposed [25], based on the Feynman path integral formulation of quantum mechanics but the analytical form is still too complicated to be of practical use.

More recently alternative approaches tend to use the methods developped for the valence bond theory when the diffraction pat-

tern exhibits a full plane of the reciprocal plane i.e., when the electron beam is aligned along low index row of the crystal (or atomic strings). The advantage of working in real space is tnat one is able to make use of the near cylindrical symmetry of the atomic strings ("muffin tin" potential). Bloch waves in two dimensions are developped either in plane wave (APW method) or in cylindrical wave with angular momentum expansion (KKR method) by Ozorio de Almeida [26] or in Gauss type orbital by Kambe [27]. Reduction of the number of beams by symmetry is also effective along the rows. Furthermore unlike the many beam matrix the KKR matrix is usually quite small because the scattering by the atomic string potential is predominantly of s and p character. This approach has given a new insight on the localized orbitals corresponding to Bloch waves bound or antibound to atomic strings [28].

Gemmel [29] and Fujimoto et al. [30] for these special orientations have used concepts of classical channeling theory of particle motion in crystals and an interesting connection has been claimed between extinction distances and oscillations of the electron in the potential well.

An algebraic approach to N-beam theory has been undertaken by A.F. Moodie [31] in the projection operation form of Sturkey's scattering matrix solution but an invertible form is at present limited to the 3-beam case.

EXPERIMENTAL POSSIBILITIES FOR ELECTRON DIFFRACTION AND IMAGING

One of the important advantages of electrons over other diffracting particles is that they are easily deviated in a controlled manner and electron optics has now attained a high degree of development bu continuous progress of the machining of lenses. Many different machines are now available the flexibility of which is sufficient to allow diffraction or imaging in different modes. Imaging mode a 2 Å level is routinely attainable and has in the five past years completely renewed the field of structure analysis by electrons. The basic transmission electron microscopy (TEM) (fig. 3) has been extended in multiple ways :

i) A large range of voltage are available from 100 keV up to 1 meV and the high voltage electron microscopy is still able to be more widely used specially at intermediate voltages.

ii) The objective lens characteristics has been optimized and very low spherical aberration coefficients are now customary.

iii) The electron gun has been optimized to produce high brightness emission. In particular the field emission gun is promised a large development in the near future.

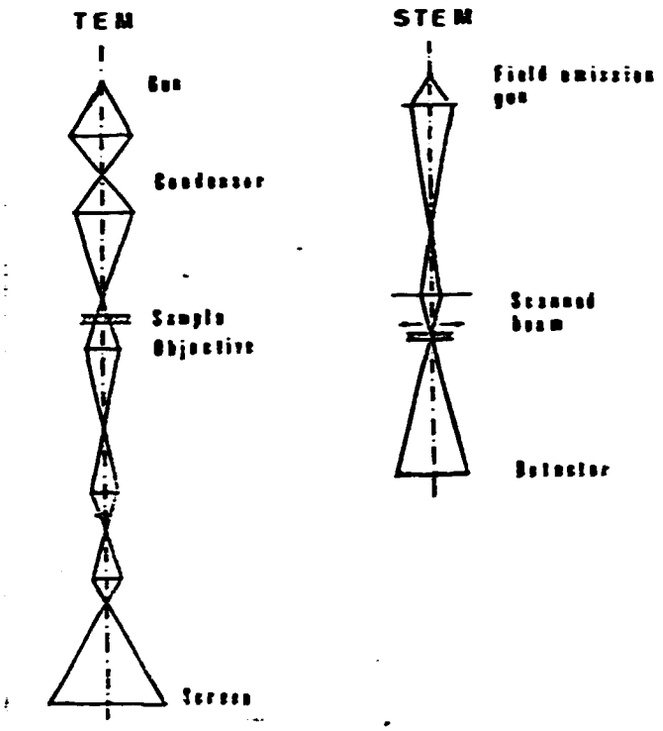

Fig. 3 - TEM and STEM schematic arrangement

In the TEM mode of operation the incident electron wave is often approximated to a plane wave as the angular divergence of the incident beam is small compare to the scattering angles. Images as well as poi t diffraction patterns are easily obtained by a simple change in the lens excitations. However the diffraction patterns are of limited value for quantitative work : thickness and orientation are rarely well controlled even on the minimum micro-diffraction area (usually $\sim$ 1 μ). With additional lenses however convergent beam conditions are also possible producing a large cone of illumination (0.5°) focussed on small area, typically (50 Å) (Fig. 4).

In the high resolution scanning transmission electron microscope (STEM) (fig. 3) firstly developped by Crewe [32] a new type of electron microscope has appeared. It consists in producing a small focussed spot of electrons (2-3 Å) which is then scanned across the specimen. Any effect produced on the beam by interaction with matter is then detected and displayed as an intensity variation on a synchroneously scanned T.V. display. In this instrument the ordinary illumination condition is a large cone angle. Images as well as diffraction patterns (especially convergent beam pattern) are also easily observable. Microdiffraction

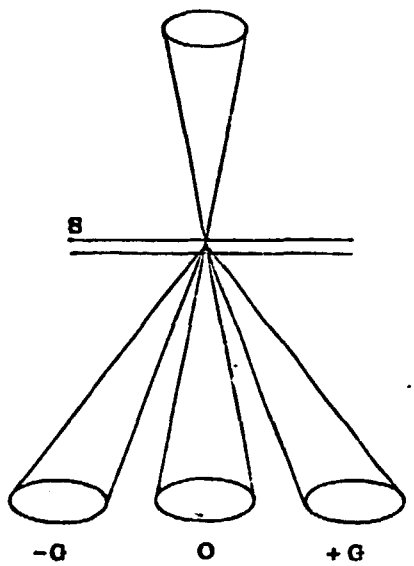

Fig. 4 - The convergent beam diffraction pattern obtained for a convergent incident beam. Only the area limited by the beam on the specimen is diffracting.

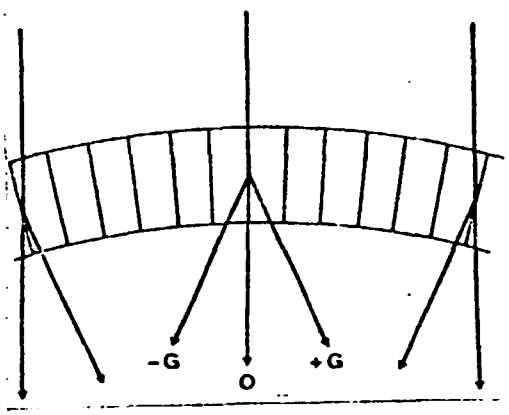

Fig. 5 - Bend contours obtained on a bend crystal. O beam intensity is varying with the position. Patterns obtained around symmetrical positions are governed by electron channeling.

from region as small as 10 Å can be recorded [33].

In TEM or STEM mode multibeam images (several diffracted beams are combined to form the image) give direct images of the projected structure of the crystal if viewed along low index row. The present state of the art is limited to a 2 Å level but 1.2 Å will be possible in the near future on a few instruments. However in principle the diffraction pattern contains information on smaller details and much effort is at present applied to extracting this information from convergent beam patterns.

STRUCTURE ANALYSIS

Some illustrative examples of structure analysis are now reviewed either in the diffraction or direct imaging mode. It must be emphasized that dynamical scattering theories have been necessary to interpret correctly the experimental results. Furthermore the high sensitivity of the dynamical conditions permits refined analysis particularly of defects in crystalline structure.

Diffraction methods

Conventional methods of structural analysis by electron diffraction have been limited to polycrystalline samples or bent crystals. There has been little progress in this field since the work of Vainshtein [1]. No real attempt has been made to calculate diffraction intensities by N-beam dynamical theories because of the large number of parameters involved (thickness, orientation, crystallite size). Kinematical or sometimes second-order approximation of Bethe are often postulated. For randomly orientated crystallites producing powder pattern special care is necessary to avoid non systematic interaction.

Localized method are, by far, much more fruitful. Convergent beam methods offer great advantages over the conventional methods: for an area limited to few hundred angströms it is easy to control the pertinent parameters. The resultant diffraction pattern is a series of disc-like spot in each Bragg direction within which the intensity distribution represents the variation of diffraction intensity with incident beam direction. Thus these patterns contain large amount of information recorded simultaneously. In contrast to the kinematical case the symmetry information is not limited by the Friedel's law and absolute symmetry determinations have been made. This allows direct detection of structural polarity and the distinction between centrosymmetry or non centrosymmetry (Goodman and Lehmpfuhl [34]). Complete space group determination is then possible : when the convergent beam zone axis pattern is taken on sufficiently thick specimen three dimensional interaction occurs and all the elements of the space group can be determined with one or two patterns (because of the upper layer interaction).

Useful information can be added from observation of Kikuchi lines in convergent beam pattern. This represents an upper layer interaction and provides additional space group information (Rackham et al [35]).

Convergent beam pattern in a modern STEM is probably even more interesting as coherence is preserved in all the diffraction disc. The diffraction discs of very limited region (down to 10 Å) will be sharply defined and as pointed out by Spence [36], will overlap if the corresponding crystal lattice spacing is resolved. The regions of overlap will have intensities varying with translation of the incident beam and with the relative phases of scattered beams. Such a method allows phase determination of all reflections in a zone within the resolution limit of the instrument.

The dynamical diffuse scattering is also commonly recorded when studying high density of defects in a crystalline matrix. The case of recording such diffuse scattering enables the study of

order-disorder, thermal motion, point defect ordering or charge density waves even on very small specimens. In particular the short range order (S.R.O.) has received much attention (D. Watanabe [37]). The diffuse scattering can be interpreted qualitatively by kinematical considerations. However for quantitative purposes dynamical diffuse scattering must be taken into account. The most commonly assumed model (Gjønnes [38]) is given by summing the amplitudes (or the intensities if there are no correlation) of the diffuse scattering given by all the individual slices taken independently, in the multislice model. Diffuse scattering of individual defects (point defect and dislocation) has been calculated by Fields and Cowley [39] using the periodic continuation construction and a full multislice method, but there are still no experimental results to take advantage of this elaborate analysis.

Imaging methods

The transmission of a perfect crystal for one particular beam (either 0 or diffracted beam) varies with the angle of the incident electron beam. This effect can be recorded in the imaging mode as illustrated in fig. 5 and is called bend contour electron microscopy (Steeds et al [40]) : this method is limited to special specimen geometries but small magnification is needed so that they are easy to obtain on ordinary electron microscopes. Images taken with a high resolution electron microscope gives direct insight in the projected structure as illustrated in fig. 6. Numerous examples [5] are now available which show applications in various fields : solid state physics, solid state chemistry, geology and biology.

For a periodic structure the image intensity is given by :

$$I(r) = \left| \sum_{o}^{g_{max}} \psi_g \exp i(\phi_g + \chi_g) \exp i2\pi \underset{\sim}{g}.\underset{\sim}{r} + \psi_o \exp i(\phi_o - \chi_o) \right|^2 \quad (15)$$

where ψ_o, ψ_g and ϕ_o, ϕ_g are the amplitudes and phases of the O beam and g diffracted beam ; g_{max} is given by the aperture function. The amplitude and phase of each beam are calculated directly in the multislice method or via the excitation of Bloch waves. χ_o and χ_g are additional phase shift due to the aberrations of the electron microscope. This phase shift is given by :

$$\chi_g - \chi_o = \frac{2\pi}{\lambda} \left(C_s \frac{g^4}{4\lambda^4} + \Delta z \frac{g^2}{2\lambda^2} \right) \quad (16)$$

where C_s is the spherical aberration of the objective lens and Δz the defocusing distance. All the art of the electron microscopist is to minimize the effect of (16) by appropriate choice of the

defocusing distance so that the image will be very close to the intensity at the specimen exit face. The conditions for which (16) is stationary over a large range of g vector is the optimum focus or Scherzer focus. The aperture function is introduced as fluctuations (mainly due to energy spread at the emission) would anyway not allow higher order g diffracted beams to interfere constructively with the central 0 beam. Depending on the gun, and on the voltage this limit is actually between 1.5 Å and 2 Å. Thus the number of Fourier coefficients is rather limited. From the intensity in the image (15), it is easy to deduce the phases of the diffracted beams and this represents a great advantage over the diffraction methods. It must be emphasized however that these phases are dynamical phases and have to be interpreted by the methods already mentionned above [41] (see fig. 2). For the optimum focus direct interpretation of the image in terms of the projected potential is very often possible. However it must be checked carefully especially for small details by image matching with computer simulations [42]. This is even more necessary for images of defects in crystals : by careful image matching on trial structures it should be actually possible to locate the atomic positions at a 0.3 Å level [23]. An example of such a computer simulation is given in fig. 7 for the defect experimentally observed in fig. 6.

INVESTIGATION OF THE "OPTICAL" POTENTIAL

Precise measurement of the "optical" potential seen by the electrons on a material is usually done by two methods :

- Intensity measurement of diffracted beams on the convergent beam pattern (precision usually of the order of 1 %).

- The critical voltage method. This method consists of measuring the voltage at which two branches of the dispersion surface touch one another. At this voltage there is an apparent vanishing of the second order Bragg reflection intensity and an associated reversal of Kikuchi line contrast. The effect is very sensitive and allows a determination of some of the Fourier components of the optical potential with a precision approaching 0.5 % [43]. On a few cases [44, 45] (graphite, MoO_3) experimental results were compared with calculated values including bond redistribution of electrons. Results on redistribution of electrons due to solid state bonding effects were also deduced in Copper [46].

Intensity distribution of flux at the exit face of the specimen has been recorded in details by Hashimoto et al [47]. Fine structure of the flux distribution, which is due to strong dynamical conditions, reproduces some of the Bloch waves bound to the atomic strings. The exact flux distribution is very sensitive to differences in the atomic number expecially for thick specimens.

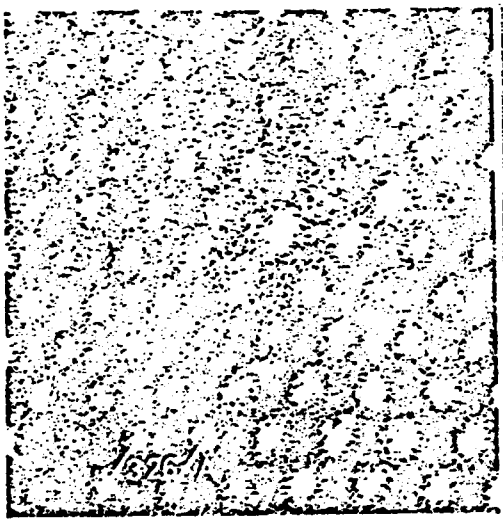

Fig. 6 - High resolution direct image of a dislocation in a germanium crystal as viewed along [011] axis. 100 keV. Thickness = 4 nm, defocusing distance = - 80 nm.

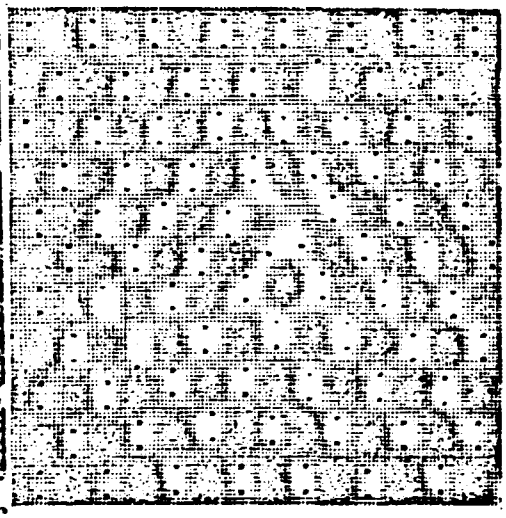

Fig. 7 - Computed image of a dislocation in a germanium crystal. Dynamical multislice calculations with 128 x 128 beams. 100 keV ; thickness = 2.5 nm defocusing distance = - 80 nm.

CONCLUSION

Although electron diffraction and imaging methods necessitate elaborate dynamical theories for correct interpretation, they are very complementary to the other structure analysis methods. The dynamical scattering should be regarded as a sensitive tool for exploring fine details either in the structural arrangement or in the electron distribution in the crystal via the "optical" potential. A good understanding of the scattering and the elaborate theory of the electron optics systems are now available and will be more widely used in the future. But the domain where electron multibeam diffraction offers a unique and definite advantage is the microlocalization. Structural details in high resolution TEM are recorded at a scale comparable with the atomic distances so that the core of defect is directly accessible and the new generation of STEM instruments will allow by microdiffraction to use the signal coming from a few hundred atoms. The flexibility of the actual instruments is also a great advantages as it allows different detection signals to be used, and chemical analysis is possible in addition to structural analysis.

REFERENCES

[1] Vainshtein B.K., Structure analysis by electron diffraction (Oxford, Pergamon) 1964

[2] Hashimoto H., Endoh H., Tanji T., Ono A., Watanabe E., J. Phys. Soc. Japan, 42 (1977) 1073

[3] Cowley J.M., Iijima S., Z. Naturforsch. 27a, (1972) 445-451

[4] Electron Diffraction 1927-1977. Inst. Phys. Conf. Ser. n° 41 (1978). The Institute of Physics Bristol and London, Ed. P.J. Dosbson, J.B. Pendry, C.J. Humphreys.

[5] Nobel symposium 47 "Direct imaging of atoms in crystals and molecules" Chemica Scripta 14 (1978-1979)

[6] Unwin P.N.T., Henderson R.J., J. Mol. Biol. 94 (1975) 425

[7] Yoshioka H., J. Phys. Soc. Japan 12 (1957) 618-628

[8] Rez P., Electron diffraction, 1927-1977, op. cit. p. 61-67

[9] Dederichs P.H., Solid Stat. Phys. 27 (1972) 135 (New York : Academic Press)

[10] Rez P., D. Phil. Thesis (1976) University of Oxford

[11] Howie A., Stern R.M., Z. Naturf. A27 (1972) 382

[12] Hall C.R., Hirsch P.B., Proc. Roy. Soc. A286 (1965) 158

[13] Darwin C.G., Phil. Mag. 27 (1914) 315

[14] Bethe H.A., Ann. Phyz., Lpz 87 (1928) 55

[15] Cowley J.M., Diffraction Physics (1975) North Holland Pub. Company, Amsterdam, Oxford

[16] Ishizuka K., Uyeda N., Acta Cryst. A33 (1977) 740-749

[17] Howie A., Whelan M.J., Proc. R. Soc. A 263 (1961) 217

[18] Hirsch P.B., Howie A., Nicholson R.B., Pashley D.W., Whelan M.J., Electron Microscopy in thin Crystals (1965) London, Butterworths

[19] Wilkens M., Phys. Stat. Sol. 6 (1964) 939

[20] Howie A., Basinski Z.S., Phil. Mag. 17 (1968) 1039-1063

[21] Anstis G.R., Cockayne D.J.H., Acta Cryst. A35 (1979) 511-524

[22] Fields P.M., Cowley J.M., Acta Cryst. A34 (1978)

[23] Bourret A., Renault A., Anstis G.R., Chemica Scripta 14, (1978-1979)

[24] Scott W.T., Rev. Mod. Phys. 35 (1963) 231-313

[25] Jap B.K., Glaeser R.M., Acta Cryst. A34 (1978) 94-102

[26] Ozorio de Almeida A.M., Acta Cryst. A31 (1975) 435-445

[27] Kambe K., Lehmpfuhl Fujimoto F., Z. Naturf. A29 (1974) 1034

[28] Buxton B.F., Loveluck J.E., Steeds J.W., Phil. Mag. 38 (1978) 259-278

[29] Gemmell D.S., Rev. Mod. Phys. 46 (1974) 129

[30] Fujimoto F., Takagi S. Komaki K., Koite K., Uchida Y., Radiat. Effects 12 (1972) 153

[31] Moodie A.F., Chemica Sripta 14 (1978-1979) 21-22

[32] Crewe A.V., Phil. Trans. Roy. Soc. Lond. B261 (1971) 61-70

[33] Cowley J.M., 37th Ann. Proc. EMSA San Antonio Texas (1979) G.W. Bailey (Ed.), p. 372-375

[34] Goodman P., Lehmpfuhl G., Acta Cryst. A24 (1968) 339-347
[35] Rackman G.M., Jones P.M., Steeds J.W., Proc. 8th Int. Cong. on Electron Microscopy Canberra (Canberra : Australian Academy of Sciences) vol. n° 1, p. 336
[36] Spence J.C.H., Scanning electron microscopy (1978) SEM Inc., AMF o'Hare IL 60666, p. 61-68
[37] Watanabe D., Inst. Phys. Conf. Ser. n° 41 (1978) op. cit. p. 88-97
[38] Gjønnes D.K., Acta Cryst. 20 (1966) 240
[39] Fields P.M., Cowley J.M., Acta Cryst. A34 (1978) 103
[40] Steeds J.W., Jones P.M., Rackman G.M., Shannon M.D., EMAG 75 (1976) Developments in Electron Microscopy and Analysis Academic Press
[41] Desseaux J., Renault A., Bourret A., Phil. Mag.35 (1977)357
[42] Bursill L.A., Wood G.J., Phil. Mag. 38 (1978) 673-689
[43] Hewat E.A., Humphreys C.J., High Voltage Electron Microscopy (1974) ed. P.R. Swann, C.J. Humphreys, M.J. Goringe (London and New York : Academic Press) pp. 52-56
[44] Goodman P., Acta Cryst. A32 (1976) 793-798
[45] Bursill L.A., Dowell W.C.T., Goodman P., Tate N., Acta Cryst. A34 (1977) 296-308
[46] Smart D.J., Humphreys C.J., in ref. 4, pp. 145-149
[47] Hashimoto H., Endoh H., Tanji T., Ona A. and Watanabe E., J. Phys. Soc. Japan 42 (1977) 1073)